Resource

Molecular Cell

Global Mapping of Herpesvirus-Host Protein Complexes Reveals a Transcription Strategy for Late Genes

Graphical Abstract

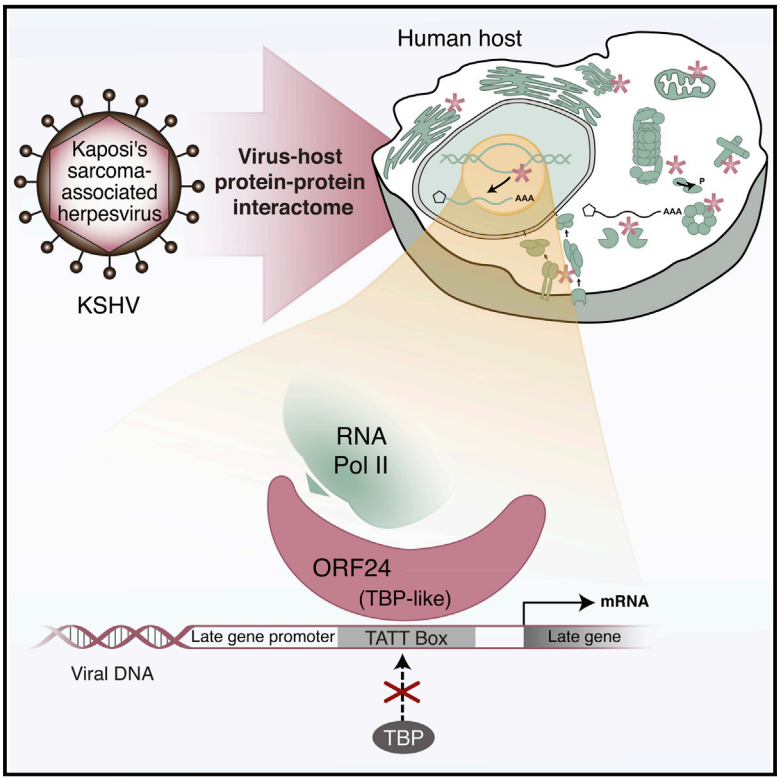

Highlights

- A herpesvirus-human protein interactome was systematically assembled in human cells
- The KSHV interaction network is a tool for predicting viral protein functions
- KSHV ORF24 recruits RNA polymerase II and replaces human TBP at late promoters

Authors

Zoe H. Davis, Erik Verschueren, ..., Nevan J. Krogan, Britt A. Glaunsinger

Correspondence

nevan.krogan@ucsf.edu (N.J.K.), glaunsinger@berkeley.edu (B.A.G.)

In Brief

Kaposi's sarcoma-associated herpesvirus (KSHV) is a major AIDS-associated pathogen. Davis et al. assemble a KSHV-host protein-protein interaction network that suggests herpesvirus-host evolutionary interplay. Using the network, they describe a hybrid KSHV-human transcription complex that activates viral late genes.

Davis et al., 2015, Molecular Cell *57*, 349–360
January 22, 2015
http://dx.doi.org/10.1016/j.molcel.2014.11.026

CellPress

Molecular Cell
Resource

Global Mapping of Herpesvirus-Host Protein Complexes Reveals a Transcription Strategy for Late Genes

Zoe H. Davis,[1,2] Erik Verschueren,[3,4] Gwendolyn M. Jang,[3,4] Kevin Kleffman,[1] Jeffrey R. Johnson,[3,4] Jimin Park,[1] John Von Dollen,[3,4] M. Cyrus Maher,[5,6] Tasha Johnson,[3,4] William Newton,[3,4] Stefanie Jäger,[3,4] Michael Shales,[3,4] Julie Horner,[7] Ryan D. Hernandez,[6] Nevan J. Krogan,[3,4,*] and Britt A. Glaunsinger[1,*]
[1]Department of Plant & Microbial Biology
[2]Division of Infectious Diseases and Immunity, School of Public Health
University of California, Berkeley, Berkeley, CA 94720, USA
[3]Department of Cellular & Molecular Pharmacology
[4]Gladstone Institutes
[5]Institute for Human Genetics
[6]Department of Epidemiology and Biostatistics
University of California, San Francisco, San Francisco, CA 94158, USA
[7]Thermo Fisher Scientific, 355 River Oaks Parkway, San Jose, CA 95134, USA
*Correspondence: nevan.krogan@ucsf.edu (N.J.K.), glaunsinger@berkeley.edu (B.A.G.)
http://dx.doi.org/10.1016/j.molcel.2014.11.026

SUMMARY

Mapping host-pathogen interactions has proven instrumental for understanding how viruses manipulate host machinery and how numerous cellular processes are regulated. DNA viruses such as herpesviruses have relatively large coding capacity and thus can target an extensive network of cellular proteins. To identify the host proteins hijacked by this pathogen, we systematically affinity tagged and purified all 89 proteins of Kaposi's sarcoma-associated herpesvirus (KSHV) from human cells. Mass spectrometry of this material identified over 500 virus-host interactions. KSHV causes AIDS-associated cancers, and its interaction network is enriched for proteins linked to cancer and overlaps with proteins that are also targeted by HIV-1. We found that the conserved KSHV protein ORF24 binds to RNA polymerase II and brings it to viral late promoters by mimicking and replacing cellular TATA-box-binding protein (TBP). This is required for herpesviral late gene expression, a complex and poorly understood phase of the viral lifecycle.

INTRODUCTION

Viruses reshape the intracellular environment during infection, both to co-opt processes necessary for viral amplification and to subvert antiviral defenses. Studies of virus-host interactions have thus provided a wealth of insight into host biology, including how the manipulation of specific pathways can contribute to disease. Due to genome size constraints, viral proteins are generally multifunctional and have evolved to target diverse cellular machinery. The number of interactions coordinated by individual viral proteomes is therefore anticipated to be substantial, as indicated by recent high-throughput proteomics analyses of virus-host protein-protein interactions (PPIs) in mammalian cells (Pichlmair et al., 2012; Rozenblatt-Rosen et al., 2012). Systems-level analyses can also reveal infection-linked patterns within cells, as well as pathways or machinery that serve as hubs for viral perturbation (Hirsch, 2010; Navratil et al., 2011).

The first comprehensive analyses of protein complexes hijacked by viruses in mammalian cells were recently documented for the RNA viruses HIV-1 and hepatitis C virus (HCV) using affinity tag/purification mass spectrometry (AP-MS), including a study by Ramage et al. (Ramage et al., 2015; Germain et al., 2013; Jäger et al., 2011a). Similar systematic mass spectrometry (MS)-based approaches have yet to be applied to DNA viruses, although a number of binary interaction screens using yeast-two-hybrid assays have been reported (Calderwood et al., 2007; Lee et al., 2011; Rajagopala et al., 2011; Uetz et al., 2006). DNA viruses can have significantly greater coding capacity relative to their RNA virus counterparts and generally exhibit genome amplification and gene-expression strategies that more closely mimic those of the host.

Herpesviruses are among the largest mammalian DNA viruses identified to date, encoding 70 to over 230 proteins. Divided into three subfamilies (α, β, and γ), herpesvirus infections have diverse pathogenic outcomes that are frequently serious in immunocompromised individuals. For example, the majority of lethal AIDS-associated cancers are caused by human γ-herpesviruses, including Kaposi's sarcoma (KS). The etiologic agent of KS is a γ-herpesvirus termed KS-associated herpesvirus (KSHV), which is also associated with the B cell lymphoproliferative disorders multicentric Castleman's disease and primary effusion lymphoma.

The KSHV life cycle is divided into lytic and latent transcriptional programs. Latency is the stage primarily linked to

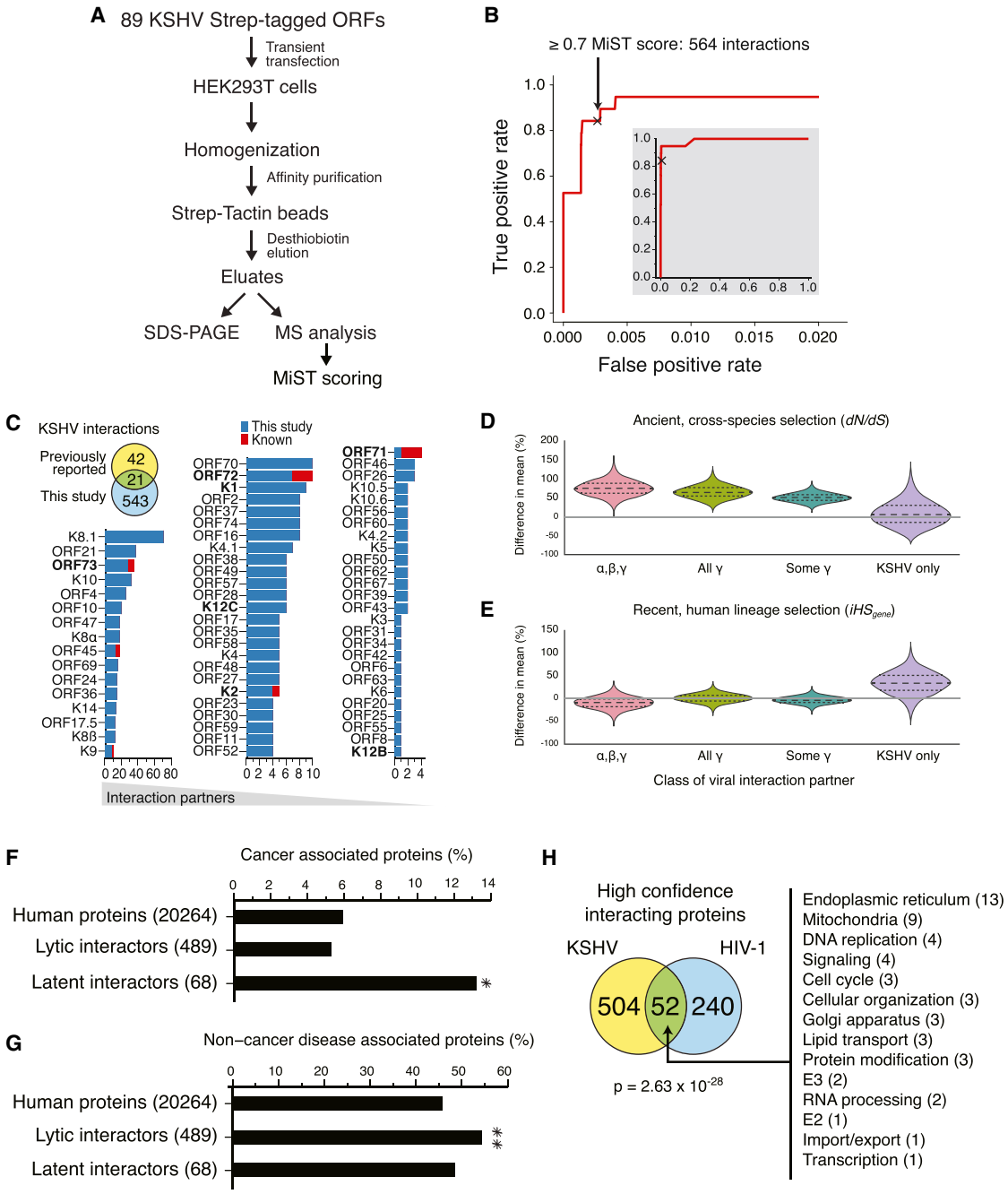

Figure 1. Assembly and Broad Characterization of the KSHV-Human Interactome

(A) Summary of the workflow used for assembly of the PPI network.

(B) The MiST feature weights and score threshold were subjected to an exhaustive parameter grid search, and the optimal values were empirically determined by maximizing the area under the curve defined by the true positive versus false-positive rate. The depicted receiver operating characteristic (ROC) curve illustrates MiST prediction accuracy with optimal feature weights for specificity (0.5) and reproducibility (0.5) with the curve inflection point marked with an x. The ROC curve was used to help define an appropriate MiST threshold of 0.7. This corresponded to 564 high-confidence interactions (see also Tables S1 and S2).

(C) Venn diagram showing the overlap between previously reported KSHV-host interactions and the high-confidence PPI network. The bar graph shows the number of host proteins associating with each viral protein, ranked in descending order, with the previously reported interactions noted in red (see also Table S2).

(D and E) Host genes that interact with viral proteins unique to KSHV show significantly elevated signs of recent selection. Shown are the distributions of mean differences from background across 10,000 bootstrap samples. Signatures of selection are measured using a mammalian-based dN/dS statistic for ancient selection (D), and the iHS statistic based on the 1000 Genomes Project for recent selection (E).

(legend continued on next page)

neoplastic disease, as the restricted subset of viral genes expressed during this phase generally manipulates growth regulatory pathways. All viral proteins are expressed during lytic replication, which is when progeny virion production occurs. Both lytic and latent KSHV infection result in broad changes in cellular metabolism and gene expression. KSHV encodes an estimated 89 proteins, including immune modulators and signaling proteins that have been "pirated" from the host, as well as proteins broadly conserved within the herpesvirus family involved in viral replication. However, the majority of KSHV-encoded proteins remain uncharacterized with a relatively small number of PPIs identified.

Here, we sought to gain a global perspective on how a large DNA virus interfaces with its host by assembling a PPI network for KSHV proteins in human cells. This network is the largest host-pathogen interactome constructed to date, as well as the first comprehensive PPI map for a DNA virus in mammalian cells. We use it to study a virus-human hybrid transcription preinitiation complex (PIC) with an essential role in directing viral late gene expression. This PIC incorporates functional mimicry of the human TATA-box-binding protein (TBP) with direct recruitment of cellular RNA polymerase II (Pol II), suggesting a system that merges principles underlying both eukaryotic and prokaryotic transcriptional regulation.

RESULTS

Assembly of the KSHV-Human Interactome

To systematically construct a comprehensive interaction network map for KSHV, we cloned each of the 89 KSHV open reading frames (ORFs) from infected cells and fused them to a strep epitope affinity tag. Protein expression was confirmed by western blotting with strep antibodies (data not shown). Where antibodies were available, we also compared the expression level of transfected viral ORFs to the endogenous version expressed during lytic KSHV infection (Figure S1A available online). The levels were generally comparable, although the level of some ORFs (e.g., K8.1) was significantly higher in the HEK293T cells, which could impact the number of interactions detected. To assemble the network, constructs were individually transfected in a minimum of three biological replicates into HEK293T cells, and viral ORFs together with their associated protein complexes were affinity purified over Strep-Tactin beads and analyzed by MS (Figure 1A). The resulting data set, assembled from over 500 AP-MS runs, contained a total of 50,835 interactions (Table S1).

A set of high-confidence PPIs was established by analyzing all interactions using the MS interaction statistics (MiST) scoring algorithm, which we designed for scoring AP-MS-derived host-pathogen PPIs (Jäger et al., 2011a; E.V., J.V.D., P. Cimermancic, N. Gulbahce, A. Sali, and N.J.K., unpublished data). MiST scores are a weighted combination of the specificity, reproducibility, and abundance features of each detected interaction. We trained the feature weights and validated our prediction accuracy on a set of published interactions to establish a MiST score of $\geq$ 0.7 for our high-confidence interaction set (Figures 1B, S1B, and S1C). A total of 21 of the 28 published interactions detected (75%, 14 trained and 7 in the validation group, $p = 7.32 \times 10^{-19}$) had MiST scores $\geq$ 0.7, demonstrating the ability of MiST to enrich for biologically relevant interactions. When applied to all detected PPIs, MiST scoring prioritized 564 KSHV-human interactions, which we refer to as the high-confidence data set (Table S1). Of the 89 KSHV proteins tested, 67 displayed high-confidence interactions with human proteins (Figure 1C). Our stringent cutoff likely excluded some biologically relevant interactions; however, the significant majority of known interactions in the data set were maintained and further revealed a multitude of previously unexplored interactions with interconnected human complexes. Indeed, comparison of this set with published KSHV-human interactions curated from the literature revealed 44% overlap (28 out of 63 published PPIs) (Table S2). We also independently validated 16 out of an attempted 28 high-confidence interactions through IP and western blotting (Table S1). While some of the interactions that failed to validate may represent false-positives, it is possible that others are nonbinary interactions that require a more limiting endogenous bridging factor.

We next looked for patterns in the KSHV interaction partners by grouping the viral proteins according to their conservation within the α-, β-, and γ-herpesviral subfamilies and analyzing the evolutionary selection profile of the interacting cellular proteins. We made the assumption that the degree of conservation of viral proteins between subfamilies reflects in part the evolutionary age of the protein, with proteins conserved among the herpesviruses likely being "older," and those unique to γ-herpesviruses or KSHV likely being "younger." We found that interactors of the more conserved viral proteins showed strong signals of ancient selection as measured by dN/dS ratios across mammals (Figure 1D). In contrast, interactors of KSHV-specific viral proteins had strong signals of recent human-specific selection as measured by iHS (Voight et al., 2006) using data from the 1000 Genomes Project (1000 Genomes Project Consortium et al., 2010), exhibiting an average increase in positive selection of 33% above background across bootstrap samples (Figure 1E). Thus, there is a dichotomy of natural selection acting broadly across mammals for interactors of ancient herpesviral proteins compared to the human-specific signatures of selection for interactors of viral proteins exclusive to KSHV. This is suggestive of a longstanding evolutionary interplay between herpesviruses and their hosts that continues to shape mammalian genomes.

A biologically relevant interaction network should be enriched for proteins linked to KSHV-induced diseases. The viral latency factors are the primary drivers of KSHV-induced cancers, although lytic cycle proteins provide paracrine signals to enhance the tumor microenvironment (Mesri et al., 2014). We therefore looked for overlap between the PPI networks of the

(F and G) Bar graphs showing the percentage of all human proteins versus the subset that interact with KSHV lytic or latent proteins that are associated with cancer (F) or noncancer diseases (G) in the DisGeNET database. * indicates a p value < 0.05, and ** indicates a p value < 0.005 as determined by the hypergeometric test (see also Figure S1; Table S3).

(H) Venn diagram depicting the overlap between the high-confidence HEK293T interaction partners of KSHV and HIV-1. The interaction partners are broken out into the number of cellular proteins in each category. The p value was determined by the hypergeometric test (see also Table S4).

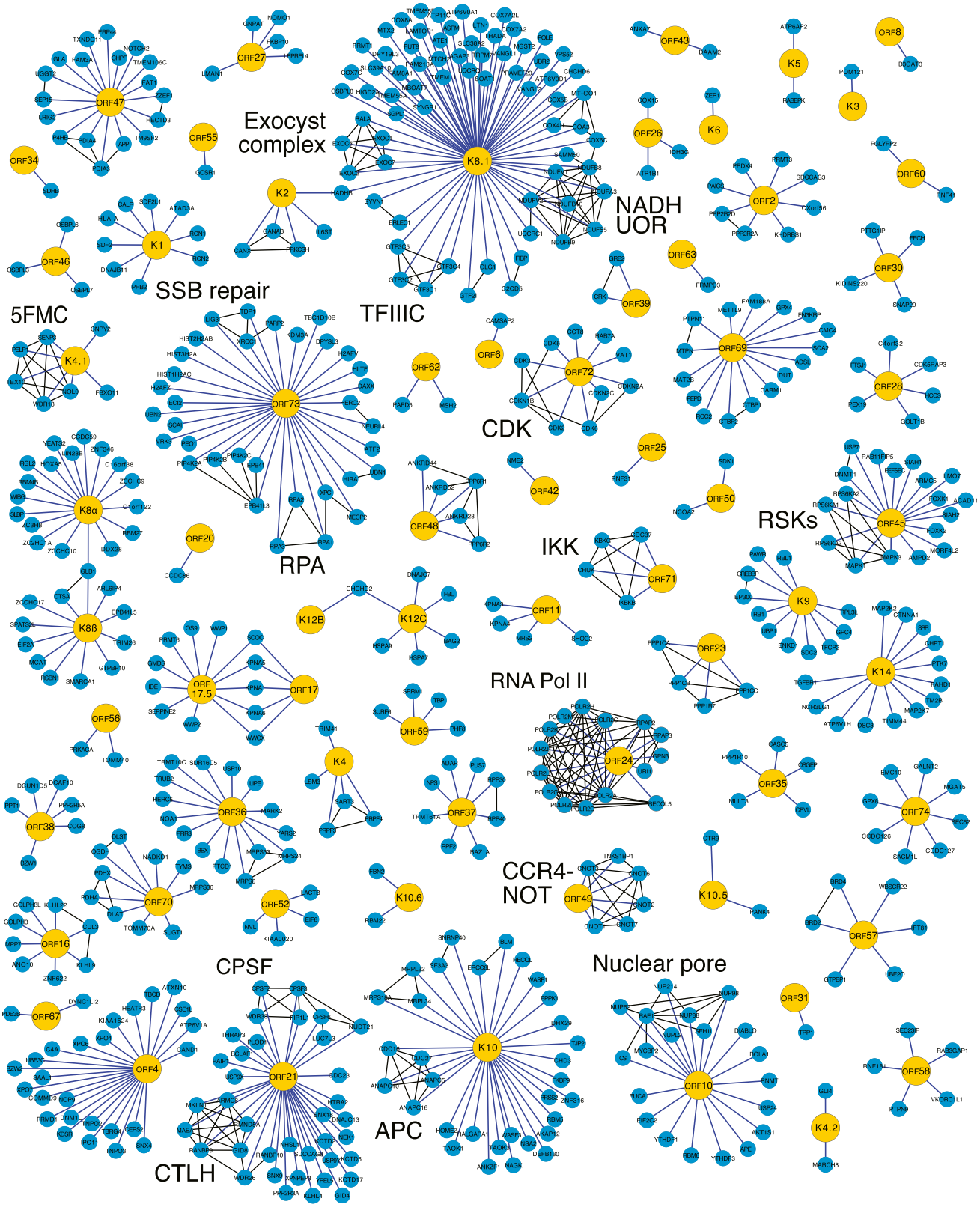

(legend on next page)

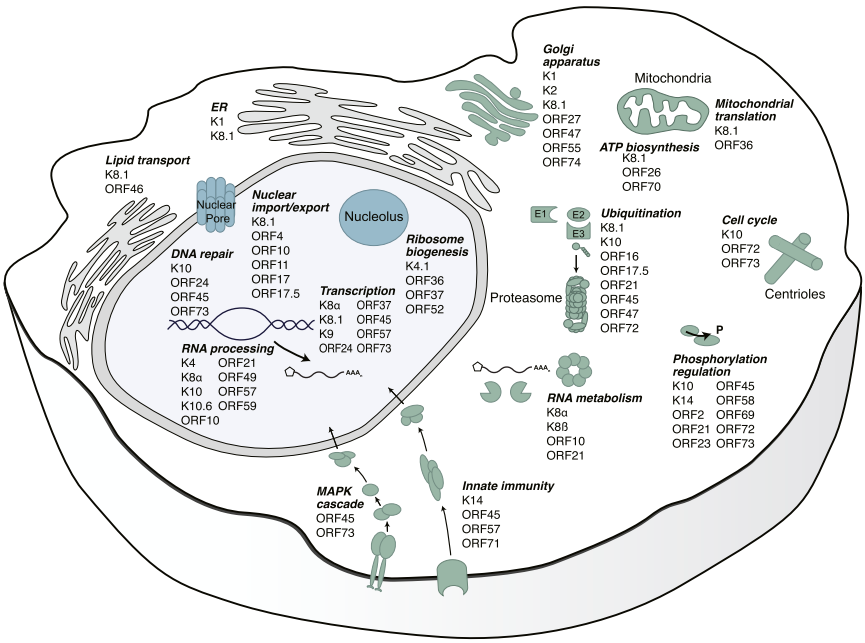

Figure 3. Using the KSHV Interactome to Predict Viral Protein Functions

Summary of predicted functions of KSHV proteins, derived from GO term and protein domain enrichments within the set of high-confidence PPIs associated with each viral protein (see also Figure S3; Tables S6 and S7).

lytic or latent proteins and disease-associated cellular proteins annotated in the DisGeNET (Bauer-Mehren et al., 2011) (Table S3) or cBioPortal (TCGA) databases. Indeed, the interaction partners of latent proteins were significantly enriched for host factors associated with cancer (Figures 1F, S1D, and S1E), whereas partners of lytic proteins were instead enriched in non-cancer disease associations (Figures 1G and S2). This correlation suggests that KSHV proteins target host factors whose disruption may contribute to disease.

KSHV and HIV-1 Proteins Have Significant Overlap in Their Interaction Partners

Epidemic KS is closely associated with patients with HIV/AIDS, and we recently assembled an HIV-1-human interactome using the same pipeline described herein (Jäger et al., 2011a). Notably, there was a significant degree of overlap in high-confidence interactors identified in both sets, with nearly all HIV-1 proteins and 22 KSHV proteins interacting with a common group of 52 cellular proteins (Figure 1H; Table S4). These overlapping proteins may be participants in cellular processes broadly required for viral amplification, or proteins selectively contributing to the KSHV-HIV-1 interaction.

The KSHV Interactome as a Tool for Functional Prediction

The high-confidence KSHV-human PPI network comprised 564 interactions among 67 viral proteins and 556 human proteins (Figure 2). When annotated to include known human-human interactions either within the network of individual viral proteins (Figure 2) or the network as a whole (Figure S2; Table S5), enrichment for components of many distinct host complexes emerged. A primary goal was to use these data to predict new protein functions, as the majority of KSHV ORFs remain uncharacterized. We therefore performed enrichment tests for gene ontology (GO) terms associated with the set of PPIs for each of the KSHV proteins (Figure S3A; Table S6). We also analyzed the individual viral PPI networks for enrichment of specific protein domains to identify functions not well annotated in the GO database (Figure S3B). The enrichment analyses accurately assigned functions to many of the characterized KSHV proteins, suggested new additional functional groupings for several of these proteins, as well as enabled us to link many of the uncharacterized KSHV proteins to specific pathways or processes (Figure 3; Table S7).

ORF24 Interaction with RNA Pol II Is Essential for KSHV Late Gene Expression

One of the most striking functional predictions was the link between the viral early lytic cycle protein ORF24 and transcription. Though unstudied in KSHV, the ORF24 orthologs in γ- and β-herpesviruses are required for the expression of viral late genes, which are transcribed only after the onset of viral genome replication (Gruffat et al., 2012; Isomura et al., 2011; Wong et al., 2007). In the high-confidence data set, exogenously expressed ORF24 copurified 10 of the 13 human RNA Pol II subunits (an additional two subunits had MiST scores above 0.6), and also with multiple Pol II subunits in lytically reactivated KSHV-positive iSLK.219 cells (Figure 4A). We engineered a FLAG tag at the N terminus of ORF24 within the KSHV genome (KSHV.FLAG.24) and found that Pol II also interacted with this endogenous ORF24 expressed from its native promoter (Figure 4B). Pol II subunits were not found in any of the other KSHV protein high-confidence networks, including well-characterized KSHV transcription factors (ORF50 and K8α) (Figure S4A; Table S1).

Figure 2. Network Representation of the KSHV-Host Interactome

The full, high-confidence interaction network contains 67 KSHV proteins (gold nodes) and 556 cellular proteins (blue nodes). Black edges indicate known interactions between cellular proteins associated with each individual viral protein. A subset of the identified complexes is labeled. NADH UOR, ubiquinone oxidoreductase; TFIIIC, transcription factor for polymerase III C; SSB repair, single-stranded break repair; 5FMC, 5 friends of methylated Chtop; CDK, cyclin-dependent kinase; RSKs, ribosomal s6 kinases; IKK, IκB kinase complex; RPA, replication protein A complex; RNA Pol II, RNA polymerase II; CPSF, cleavage and polyadenylation specificity factor complex; APC, anaphase-promoting complex; CTLH, C-terminal to LisH motif complex (see also Figure S2; Table S5).

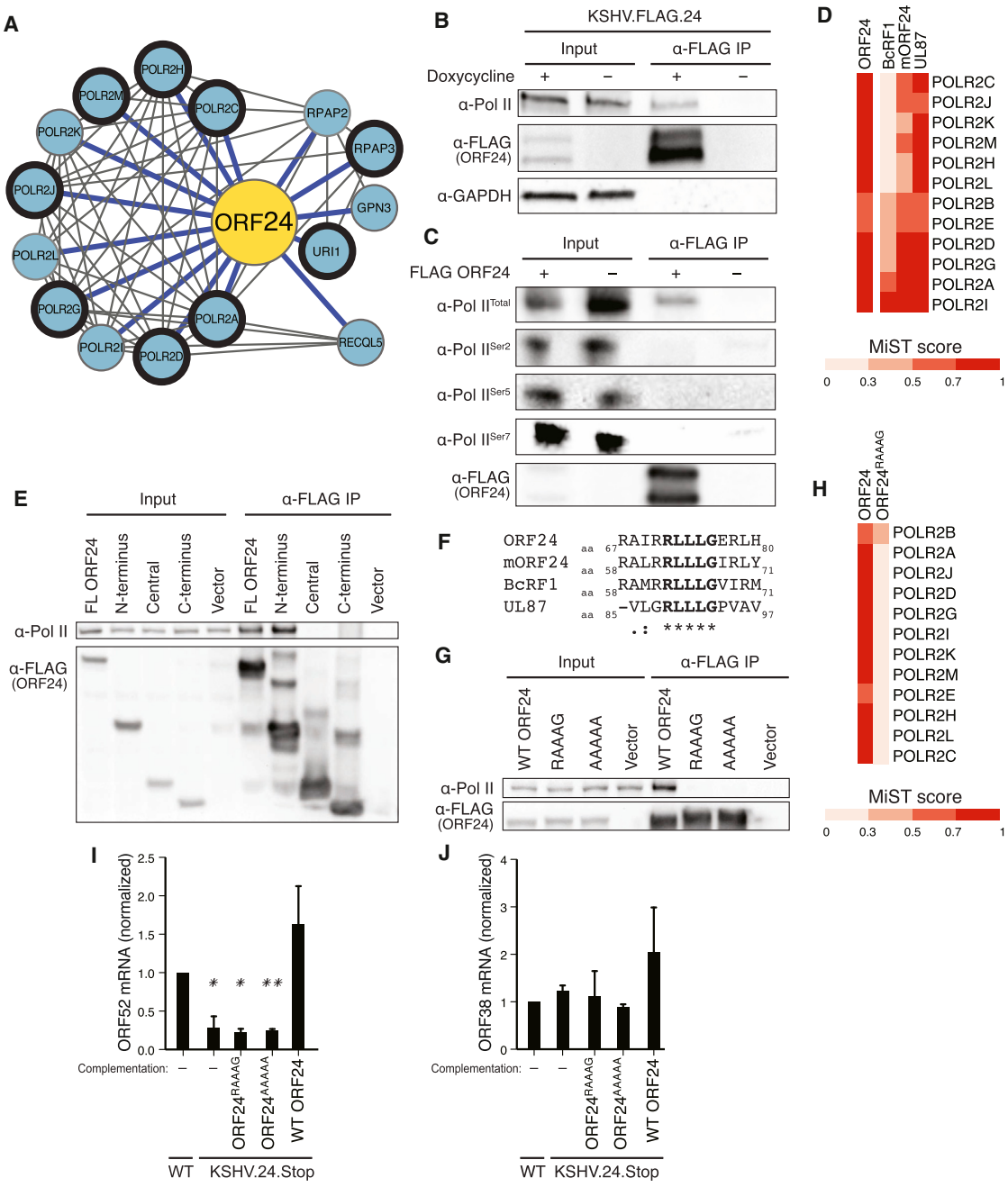

Figure 4. KSHV ORF24 Binds Human RNA Polymerase II to Drive Viral Late Gene Expression

(A) Network showing the high-confidence interaction partners of ORF24 identified in HEK293T cells (all blue nodes) and those also identified in KSHV-infected iSLK.219 cells (blue nodes with heavy black borders). Pol II subunits are depicted to the left of the ORF24 node, while Pol II accessory factors are shown to the right. Gray lines indicate known interactions between human proteins.

(B) Lysates of iSLK cells either latently (– doxycycline) or lytically (+ doxycycline) infected with KSHV.FLAG.24 were subjected to α-FLAG IP and western blotted for the RPB1 subunit of Pol II. GAPDH was used as a loading and IP specificity control. In this and all subsequent IPs, input represents 5% of lysate used for IP.

(C) Lytically induced iSLK cells infected with KSHV.WT were transduced with FLAG-tagged ORF24, and lysates were subjected to α-FLAG IP and western blotted using antibodies against total RPB1 (Pol II) or the hyperphosphorylated forms of Pol II.

(D) Heat map representing the MiST scores for Pol II subunits detected in association with the ORF24 orthologs from KSHV (ORF24), MHV68 (mORF24), EBV (BcRF1), and CMV (UL87) via AP-MS from HEK293T cells.

(E) 293T cells were transfected with plasmids expressing FLAG-tagged full-length (FL) ORF24 or fragments of ORF24 encompassing the N terminus (aa 1–401), central domain (aa 402–603), or C terminus (aa 604–752). Cell lysates were subjected to α-FLAG IP and western blotted for the RPB1 subunit of Pol II.

(F) A Clustal Omega multiple sequence alignment for the ORF24 orthologs showing the stretch of five conserved residues within their N termini.

(legend continued on next page)

ORF24 specifically bound the lower mobility, hypophosphorylated form of the RPB1 (POLR2A) subunit of Pol II, and not the form phosphorylated at serine 2, 5, or 7 of the RPB1 C-terminal domain, consistent with a potential role in PIC assembly (Figure 4C). The interaction was DNA independent, suggesting that it may occur prior to Pol II recruitment to promoters (Figure S4B). Finally, we observed that Pol II binding, as measured both by AP-MS and IP-western blotting, was a feature conserved among ORF24 orthologs in human cytomegalovirus (HCMV; UL87), Epstein-Barr virus (EBV; BcRF1), and murine γ-herpesvirus 68 (MHV68; mORF24) (Figures 4D and S4C–S4F).

KSHV ORF24 is a 752 amino acid (aa) protein with a central 209 aa domain that is highly conserved among its orthologs and is flanked by more divergent N- and C-terminal regions. Truncation mutants of KSHV ORF24 encompassing each of these domains demonstrated that the Pol II interaction was mediated exclusively through the N terminus (aa 1–401) (Figure 4E). Although the aa sequence of the N-terminal domain is poorly conserved, it does contain an invariant five aa stretch (Figure 4F). Mutation of these five aa in KSHV ORF24 to alanines (ORF24^{AAAAA}), or just the three leucines to alanines (ORF24^{RAAAG}), completely abrogated the interaction with Pol II (Figures 4G and 4H).

Similar to previous observations in EBV, CMV, and MHV68 (Gruffat et al., 2012; Isomura et al., 2011; Wong et al., 2007), introduction of a stop codon in the KSHV ORF24 locus (KSHV.24.Stop) impaired late gene expression, but did not impact early gene expression or viral DNA replication (Figures S4G, S4H, and S5A). As expected, repair of the stop mutation in the virus or complementation with wild-type (WT) ORF24 restored late gene expression (Figures S4G and S5A). When WT or Pol II binding mutants of ORF24 were exogenously expressed in cells infected with KSHV.24.Stop (Figure S4I), expression of WT ORF24, but not the Pol II binding mutants, restored expression of both the ORF52 (Figure 4I) and other late genes (Figure S5A), but did not impact expression of the ORF38 early gene (Figure 4J). Furthermore, cells complemented with the ORF24 Pol II binding mutants produced no detectable infectious virions in supernatant transfer assays (Figure S5B). Thus, the ORF24-Pol II interaction is essential for the selective activation of late genes and completion of the viral lifecycle.

ORF24 Functionally Resembles Cellular TBP

Mapped late gene promoters are strikingly minimal, as they encompass only 12–15 bp in total and are comprised of little more than a core TATA-like element (TATT) (Homa et al., 1988; Tang et al., 2004; Wong-Ho et al., 2014). The central conserved domain in the ORF24 orthologs was predicted to adopt a TBP-like secondary structure, although the proteins lack significant sequence identity (Wyrwicz and Rychlewski, 2007). Similar to the EBV and MHV68 ORF24 orthologs (Gruffat et al., 2012; Wong-Ho et al., 2014), purified KSHV ORF24 bound to a TATT-containing KSHV K8.1 late gene promoter sequence in DNA gel-shift assays, but failed to bind a size-matched segment from the KSHV ORF57 early gene promoter containing a canonical TATA box (Figure 5A). K8.1 promoter binding was dependent on its core TATT sequence, as mutating these bases to CCCC abrogated the interaction (Figures 5A and S5C).

TBP has asparagine and valine residues within its inner "saddle" that contact DNA and contribute to its specificity for the TATA sequence (Kim et al., 1993). Mutation of these positionally conserved residues in KSHV ORF24 (ORF24$^{N425A,\ N427A}$ and ORF24$^{N518A,\ N520A}$) did not impair Pol II binding, but abrogated the interaction with the K8.1 late gene promoter as well as the ability to rescue late gene expression and virion production during infection with the KSHV.24.Stop virus (Figures 5A–5C, S5A, and S5B). Thus, KSHV ORF24 is a modular protein containing at least two essential, but genetically separable, domains required to drive selective transcription from minimalistic viral late promoters.

ORF24 Replaces TBP in the Viral Late Gene PIC

TBP and TBP-associated factors (TAFs) collectively comprise TFIID, which binds the core promoter and serves as a platform for the recruitment of other PIC components. Our data suggested, however, that Pol II might be recruited independently of TFIID to viral late promoters by ORF24.

In agreement with our in vitro binding results, chromatin immunoprecipitation (ChIP) assays showed FLAG-ORF24 bound to the K8.1 late gene promoter, but not the ORF57 early gene promoter, in lytically reactivated iSLK cells infected with KSHV.FLAG.24 virus (Figure 6A). In contrast, TBP was present at the ORF57 early promoter, but not detectable at the K8.1 late promoter (Figure 6A). Unlike Pol II, both TBP and ORF24 remained at their associated promoter (Figure 6A). The apparent mutually exclusive binding of ORF24 and TBP suggests that ORF24 acts as a replacement for TBP on late gene promoters.

Cellular TBP does not bind Pol II directly; its interaction with Pol II at the PIC is instead bridged by TFIIB and other general transcription factors (GTFs) (Bushnell et al., 2004). However, these additional PIC components were absent from the KSHV ORF24 MS data, a finding we independently confirmed by western blotting for TBP, TFIIB, TFIIE, TFIIF, and TFIIH in KSHV.FLAG.24 immunoprecipitates (Figure S6A). Thus, either the recruitment of Pol II to late promoters by ORF24 bypasses the need for additional GTFs, or, alternatively, GTF assembly into the late promoter PIC occurs in a TBP-independent manner. We addressed these possibilities by measuring the in vivo

(G) 293T cells were transfected with plasmids expressing FLAG-tagged WT ORF24 or an ORF24 mutant in which the conserved "RLLLG" motif was mutated to "RAAAG" or "AAAAA." Lysates were subjected to α-FLAG IP and western blotted with the indicated antibodies.

(H) Heat map representing the MiST scores for Pol II subunits detected in association with WT ORF24 (ORF24) versus the ORF24^{RAAAG} mutant via AP-MS from HEK293T cells.

(I and J) iSLK cells infected with WT KSHV or KSHV lacking ORF24 (KSHV.24.Stop) were transduced with a retroviral vector expressing either WT ORF24 or the indicated ORF24 Pol II binding mutants. After 48 hr of lytic reactivation, accumulation of the ORF52 late gene (I) or the ORF38 early gene (J) was measured by RT-qPCR and normalized to levels of 18S, with the viral mRNA levels present during WT infection set to 1. * indicates a p value < 0.05, and ** indicates a p value < 0.005 as determined by Student's t test (see also Figure S4).

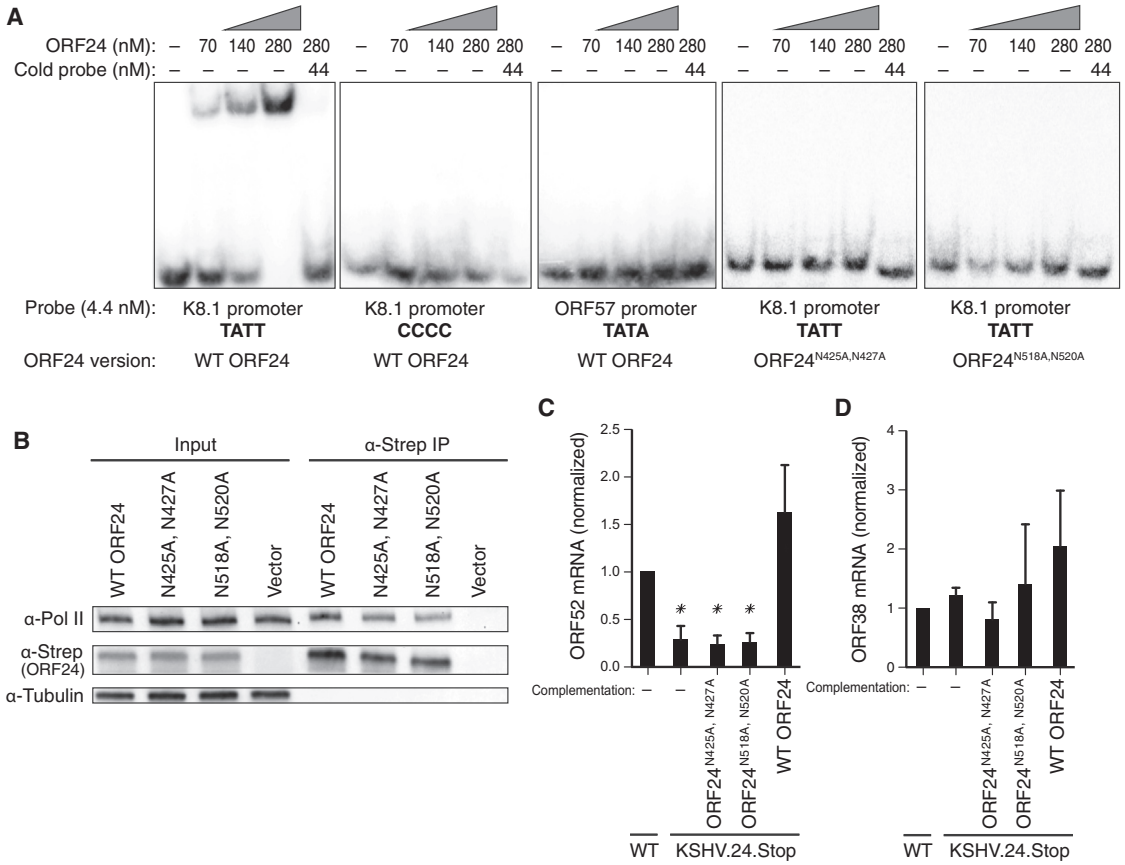

Figure 5. ORF24 Binds Late Gene Promoter DNA in a Manner Essential for Late Gene Expression

(A) Purified WT ORF24 or ORF24 putative DNA-binding mutants (ORF24$^{N425A,\ N427A}$ and ORF24$^{N518A,\ N520A}$) (0–280 nM) were subjected to EMSA with 23 nt radiolabeled dsDNA probes encompassing the K8.1 late promoter, which contains a central "TATT" sequence, or the ORF57 early promoter, which contains a central "TATA" sequence. Where indicated, the "TATT" motif in the K8.1 promoter probe was mutated to "CCCC." The specificity of the interaction was confirmed by competition with unlabeled (cold) probe.

(B) HEK293T cells were transfected with plasmids expressing strep-tagged WT ORF24 or the indicated ORF24 DNA-binding mutants. Lysates were subjected to α-strep IP and western blotted for the RPB1 subunit of Pol II. Tubulin was used as a loading and IP specificity control.

(C and D) iSLK cells infected with WT KSHV or KSHV.24.Stop were transduced with a retroviral vector expressing WT ORF24 or the indicated ORF24 DNA-binding mutants. After 48 hr of lytic reactivation, accumulation of the ORF52 late gene (C) or the ORF38 early gene (D) was measured by RT-qPCR and normalized to levels of 18S, with the viral mRNA levels present during WT infection set to 1. * indicates a p value < 0.05 as determined by Student's t test (see also Figure S5).

promoter occupancy of the GTFs TFIIB and TFIIH (ERCC3), two canonical components of PICs found at RNA Pol II-transcribed promoters (Figure 6B). Despite the absence of TBP, ChIP assays revealed assembly of both TFIIH and TFIIB on the K8.1 late gene promoter (Figure 6B). TFIIB occupancy at the K8.1 promoter was lost in the KSHV.24.Stop virus, confirming that recruitment of at least a subset of GTFs to this promoter is ORF24 dependent (Figure S6B). Thus, the KSHV ORF24 protein nucleates assembly of a PIC that bypasses the need for TBP, but is nonetheless structured to enable subsequent recruitment of other core mammalian transcription factors.

DISCUSSION

Here, we present the largest whole virus-host interactome defined to date. Host genes that interact with more highly conserved viral proteins show significantly elevated rates of positive selection across mammals. This effect diminishes for the more recently evolved KSHV-specific viral proteins, consistent with restricted contact across the expanses of the host-pathogen phylogenetic trees. However, the interactors of these KSHV-specific proteins show a dramatic increase in signatures of recent natural selection within human populations. We therefore speculate that KSHV may have contributed to shaping patterns of human genetic variation over the last 10,000–30,000 years.

There is significant overlap between the virus-host interactomes of KSHV and HIV-1, with high-confidence targets of nearly every HIV-1 protein present in the overlapping PPI set. This overlap is notable because, although these two viruses are pathologically linked (particularly in the case of KSHV-induced diseases), they have distinct life cycles and replication strategies. As more systematic interaction data sets emerge, it will be of interest to examine whether any of these overlapping partners are present within additional virus-host interactomes. In this regard, core

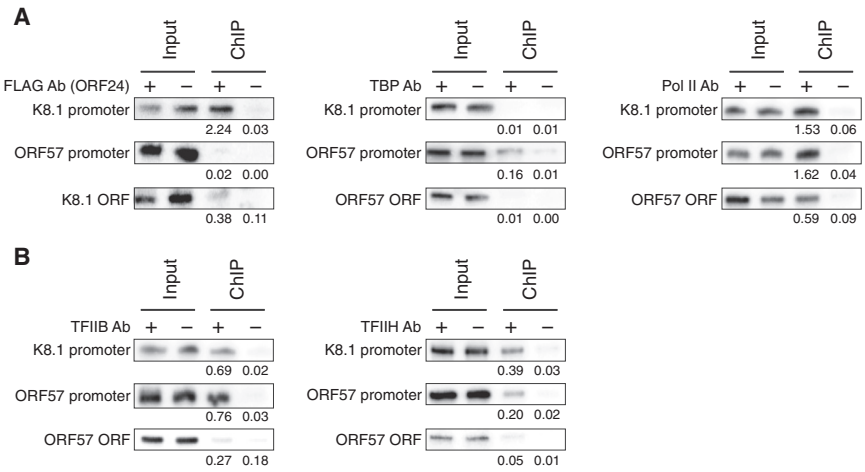

Figure 6. ORF24 Functionally Replaces TBP on the Late Promoter

(A and B) Chromatin from iSLK cells lytically infected with KSHV.FLAG.24 was isolated and subjected to ChIP using antibodies against FLAG (to precipitate FLAG ORF24), TBP, and Pol II (A), or TFIIB and TFIIH (ERCC3) (B). Coprecipitating DNA was detected by PCR using radiolabeled nucleotides and primers specific for the indicated promoter or gene body. Experiments were repeated at least three times, and a representative image is presented with the ChIPs quantified against input samples (see also Figure S6).

host pathways that are reiteratively targeted by invading pathogens could generate signals akin to ''patterns of pathogenesis'' that are recognized by the innate immune system as markers of viral infection (Vance et al., 2009).

There are several strengths in our systematic approach that lead to a robust PPI network. First is our ability to identify reproducible and specific interactions, which should serve as the basis for future hypothesis-driven studies to probe their role in the KSHV life cycle. We demonstrated that the PPI network could accurately predict known protein functions and, in the case of viral latency factors, was enriched for proteins linked to cancer. Our standardized pipeline also eliminates the inherent difficulties in cross-comparisons of individual PPI experiments. That said, the network likely underestimates the number of interactions coordinated by KSHV. It does not capture PPIs driven by complexes comprised of multiple viral proteins and excludes some biologically relevant interactions that were detected but deprioritized by MiST due to low specificity.

Directed by the interactome, we gained insight into a poorly understood stage of γ-herpesvirus gene expression (Figure 7). Late genes of all DNA viruses become transcriptionally active only after the onset of viral DNA replication and produce proteins necessary for progeny virion assembly. Foundational work in related herpesviruses has revealed a complex of six viral proteins to be essential for late gene expression and recruitment of Pol II (Arumugaswami et al., 2006; Aubry et al., 2014; Jia et al., 2004; Perng et al., 2014; Wong et al., 2007; Wu et al., 2009). Although the precise roles of each of these factors remain unknown, the ORF24 orthologs in related herpesviruses have been shown to exhibit sequence-specific DNA-binding activity and display predicted structural homology to TBP (Gruffat et al., 2012; Wyrwicz and Rychlewski, 2007). We find that ORF24, but no other KSHV protein, binds Pol II, indicating that it is the late gene transcription factor that mediates polymerase recruitment to KSHV late promoters. Furthermore, the observation that ORF24, but not TBP, occupies the KSHV K8.1 late promoter in vivo suggests that ORF24 functionally replaces TBP specifically at late gene PICs. This interaction occurs through the atypical TATA box (TATT) characteristic of late promoters and requires ORF24 residues that are spatially and functionally similar to the DNA-binding residues of TBP. These data support the hypothesis that KSHV ORF24 and its orthologs function as the first described viral TBP mimics (Wyrwicz and Rychlewski, 2007), orchestrating the assembly of an atypical virus-host hybrid transcription complex.

TBP serves as a critical nucleation factor for PIC assembly, including at promoters lacking a TATA box (Thomas and Chiang, 2006). However, unlike ORF24, TBP does not directly bind Pol II; the polymerase is instead brought to the TBP-bound promoter through interactions with TFIIB and additional transcription-associated factors (Murakami et al., 2013). The low degree of sequence homology between ORF24 and TBP makes it unlikely that ORF24 is able to associate with a similar cohort of TAFs and GTFs, a notion supported by the selectivity of the ORF24-Pol II interaction. Thus, cellular GTF recruitment to late promoters may instead occur through other viral or cellular proteins that perhaps join the ORF24-bound DNA. ORF24-directed recruitment of Pol II could also enable late genes to bypass select regulatory factors required for canonical eukaryotic promoter activation.

While proteins from other viruses have been reported to interact with Pol II, ORF24 is unique in its ability to coordinately bind Pol II and promoter DNA (Dorjsuren et al., 1998; Engelhardt et al., 2005; Mavankal et al., 1996; Takramah et al., 2003; Zhou and Knipe, 2002). This is reminiscent of prokaryotic sigma factors, which compete to bind the RNA polymerase holoenzyme and are required for selective promoter recognition and initiation (Österberg et al., 2011). It is possible that herpesviruses have evolved an analogous strategy to secure sufficient levels of Pol II for strong late gene expression late in infection, a time when the cell is stressed and perhaps constrained for resources. DNA viruses likely display significant variety in PIC composition, including in the core GTFs as has been shown for some cell cycle-regulated promoters (Guglielmi et al., 2013). Future studies of the regulation of late genes are therefore anticipated to uncover other alternative modes of transcriptional regulation with parallels in mammalian cells.

EXPERIMENTAL PROCEDURES

Plasmid Construction

A library of strep-tagged KSHV ORFs was assembled from RNA from TREx BCBL-1-RTA cells reactivated for 36 hr with TPA (20 ng/ml), ionomycin

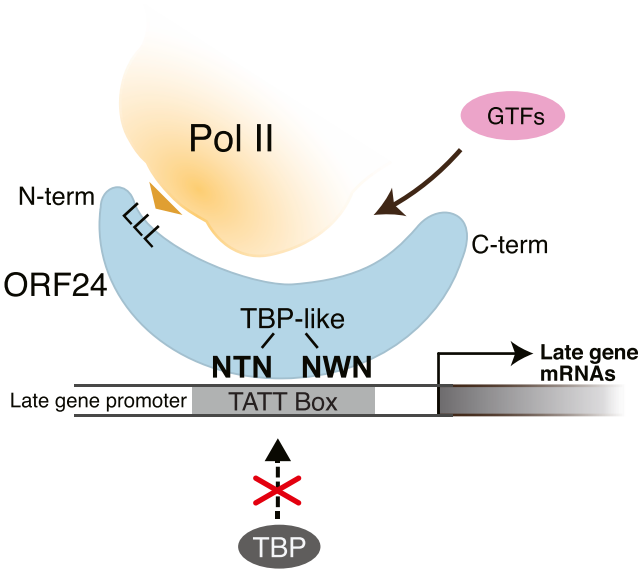

Figure 7. Model for ORF24 Activation of Late Gene Promoters
ORF24 interacts with Pol II through conserved leucines in its N-terminal domain. The polymerase is then brought to the late promoter TATT box via the ORF24 TBP-like domain. TBP is excluded from late promoters, and instead ORF24 binding nucleates assembly of the PIC by enabling recruitment of other cellular GTFs.

(500 ng/ml), and doxycycline (1 μg/ml). ORF primers were designed based on sequences from the European Nucleotide Archive and GenBank. Inserts were ligated into pcDNA4/TO (Invitrogen) modified to include a C-terminal 2× strep tag. Additional cloning and primers including restriction sites for all ORFs cloned in this study are listed in Supplemental Experimental Procedures.

Cell Culture and Transductions

HEK293T (ATCC), Phoenix 293 retroviral packaging cells (Swift et al., 2001), the renal carcinoma cell line iSLK puro (Sturzl et al., 2013) bearing a dox-inducible version of the major KSHV lytic transactivator RTA, KSHV-positive iSLK.219 cells (Myoung and Ganem, 2011), and other iSLK puro-derived cell lines were maintained in Dulbecco's modified Eagle medium (DMEM; Invitrogen) with 10% fetal bovine serum (FBS; Invitrogen, HyClone) and penicillin-streptomycin (Invitrogen). The BJAB B cell line was maintained in RPMI (Invitrogen) medium with 10% FBS and penicillin-streptomycin. Stable cell lines expressing tagged viral ORF24 for affinity purification or ORF24 complementation assays were generated by retroviral transduction.

Affinity Purification and Western Blotting

Affinity purification of proteins to be analyzed by MS was performed as previously described (Jäger et al., 2011a, 2011b). Briefly, clarified cell lysate was incubated with prewashed Strep-Tactin beads (IBA) or FLAG beads (Sigma) and allowed to bind for 1–3 hr. Following purification, complexes bound to beads were washed and then eluted with desthiobiotin (IBA) or 3X FLAG peptide (Elim Biopharm) for strep or FLAG tags, respectively.

MS

Eluates were processed, trypsin digested, and concentrated for LC-MS/MS. Digested peptide mixtures were analyzed by LC-MS/MS on a Thermo Scientific Velos Pro ion trap MS system equipped with a Proxeon EASY nLC II high-pressure liquid chromatography and autosampler system.

Network Scoring and Benchmarking

Weights of the three MiST features were set by supervised training using two-thirds of the known KSHV-host interactions detected in our screen as a positive set (19/28), 100-times-larger random subsets of the interactome as negative sets, and the remaining third of known interactions as a validation set (9/28). An exhaustive grid search was performed on the 4D vector described by the three weight variables and a threshold variable. The domain of these variables was limited to between 0 and 1, with 0.01 increments. The sum of the three variables was constrained to 1. For every complete assignment of the vector, the true positive rate (TPR) and false-positive rate (FPR) in the set of MiST scores higher than the threshold were computed against the high-confidence training and validation set or the negative set, respectively, together with the AUC for these rates. The feature weight values that gave rise to a maximal AUC, low FPR, and maximal TPR on the validation set were selected as the final MiST weights for abundance, reproducibility, and specificity. Network representations were plotted using Cytoscape v. 2.8.3 (Smoot et al., 2011).

Evolutionary Analysis

Human proteins interacting with only one KSHV protein were binned according to the classification of their viral binding partner within the herpesviral subfamilies. Within these bins of human proteins, differences in evolutionary pressures compared to a random background of MS-observable human proteins were assessed. Cross-species selection (dN/dS) was assessed based on multiple sequence alignments of human, chimp, gorilla, orangutan, and rhesus macaque sequences constructed using MOSAIC (Maher and Hernandez, 2014). iHS scores were calculated by selscan (Szpiech and Hernandez, 2014), then summarized at the gene level by taking a linear combination of the log of the number of nominally significant z-scores and the maximum z-score within a given coding region. Weighting was chosen using principle components analysis.

Disease Association Analysis

All proteins in the reference proteome were labeled as "cancer-associated," "other disease associated," or "none" based on their DisGeNET disease annotations. The reference proteome was divided in three sets: all proteins, latent KSHV ORFs (K1, K2, K12A, K12B, K12C, ORF71, ORF72, and ORF73) interacting proteins, or lytic KSHV ORFs (remaining). Using this partitioning, relative fractions of proteins with cancer associations or other disease associations were computed, and the significance of the observed counts was computed with the hypergeometric test.

Ontology Enrichment Analysis of Prey Proteins

For each analysis, the list of identified preys was joined with the respective ontology mapping using UniProt accession codes. Then, for each ontology term in this joined list, the average MiST score of all associated prey proteins was compared against a sampled distribution of averages for equally sized random subsets of the data. The probability that the observed term score was higher than the distributed sampled average was computed by the one-tailed cumulative normal distribution test. The set of enrichment p values for all terms in the ontology mapping was adjusted for multiple hypotheses testing by applying the Benjamini-Hochberg correction (also known as FDR control or q value). Terms that were significant at an FDR of 0.05 were reported as output.

KSHV Mutagenesis

KSHV mutants were engineered using KSHV BAC16 mutagenesis as previously described using a two-step scarless Red recombination system (Brulois et al., 2012). iSLK-derived cells used in this study include a BAC with a premature stop codon in the ORF24 coding region (KSHV.24.Stop) and an N-terminally FLAG-tagged ORF24 (KSHV.FLAG.24).

RT-qPCR

RNA isolated from the relevant lytically reactivated iSLK puro-derived cells was treated with Turbo DNase (Ambion) and reverse transcribed with AMV RT (Promega) using random 9-mers or gene-specific primers in cases of overlapping viral transcripts. cDNA levels were quantified using DyNAmo color flash SYBR green master mix, ROX passive reference dye (Thermo Scientific), and transcript-specific primers. Transcript levels were normalized to 18S. Error bars represent the SD of three independent experiments.

ChIP

iSLK cells containing WT or mutant KSHV were induced with 1 μg/ml doxycycline for 36 hr before harvesting chromatin. ChIP was performed as described (Listerman et al., 2006), but using a Covaris focused sonicator to shear chromatin. After reversing crosslinks, DNA was purified and eluted in 150 μl of ddH_2O. Eluted DNA (0.5–1 μl) was subjected to 20–25 cycles of PCR in reactions spiked with α-^{32}P dCTP. PCR products were resolved on urea PAGE gels, quantified using Image Lab (Bio-Rad) software, and normalized to 1% input.

Electromobility Shift Assays

WT or DNA-binding mutants of 3X FLAG ORF24 were isolated from transduced BJABs in lysis buffer (100 mM HEPES [pH 7.9], 500 mM NaCl, 1% NP-40), affinity purified over FLAG beads, and eluted with 3X FLAG peptide. Protein purity was assessed by silver stain. Samples were dialyzed against 20 mM HEPES (pH 7.9), 40% glycerol, 100 mM KCl, 0.5 mM DDT, and 0.5 mM PMSF. Shift buffer (1 μg/μl salmon sperm DNA, 0.5 mg/ml BSA, 0.05% Triton X-100, 10% glycerol, 10 mM HEPES [pH 7.9], 40 mM KCl, 5 mM $MgCl_2$, and 10 μM BME) was added to binding reactions containing 70–280 nM protein and 4.4 nM radiolabeled probe. Oligonucleotides were end-labeled with γ-^{32}P ATP using T4 PNK (NEB) and purified, and reverse-complemented sequences were annealed together to make a double-stranded probe. Reactions were incubated at 37°C for 30 min and resolved by native PAGE.

SUPPLEMENTAL INFORMATION

Supplemental Information includes six figures, seven tables, and Supplemental Experimental Procedures and can be found with this article online at http://dx.doi.org/10.1016/j.molcel.2014.11.026.

AUTHOR CONTRIBUTIONS

Z.H.D. cloned and expression tested the KSHV ORF library, assisted with analysis of the interactome dataset, and performed all experiments related to KSHV ORF24. E.V. and J.V.D. ran bioinformatics and statistical analysis of the interactome data. G.M.J. and S.J. affinity purified KSHV ORFs from human cells for MS. K.K. assisted with generation of the KSHV ORF library. J.R.J., T.J., W.N., and J.H. were involved in MS analysis. J.P. assisted with ORF24 cloning and construction of KSHV mutants. M.C.M. and R.D.H. performed evolutionary analysis. T.J. and W.N. assisted with affinity purification of the KSHV ORFs. M.S. assisted with figure design and graphics. N.J.K. and B.A.G. oversaw all experiments and assisted with data interpretation. Z.H.D., E.V., N.J.K., and B.A.G. wrote the paper.

ACKNOWLEDGMENTS

We would like to thank the members of the B.A.G. and N.J.K. labs and Laurent Coscoy for helpful discussions and critical reading of the manuscript. We would also like to thank Christopher Hann-Soden, Alexandre Mercier, Trever Greene, Andrew Birnberg, Matthew Gardner, Marta Gaglia, and Edward Tang for help with cloning, cell culture, and MS; Jeffrey Queisser for computational help; and Sumit Chanda for ORFeome constructs. This research was supported by NIH R01 grants CA160556 and CA136367 and CHRP IDEA award ID13-B-529 to B.A.G., NIH P50 GM082250, P50 GM081879, PO1 AI090935, PO1 AI091575, PO1 CA177322, U54 AI081680, and DARPA-10-93-Prophecy-PA-008 grants to N.J.K., R01HG007644 and a Sloan Foundation Research Fellowship to R.D.H., an Irving H. Wiesenfeld Fellowship to Z.H.D., and a UCSF M. Lloyd Kozloff fellowship and NIH F31 CA180609-01 to M.C.M. N.J.K. and B.A.G. are WM Keck Foundation Young Investigators.

Received: April 16, 2014
Revised: August 20, 2014
Accepted: November 21, 2014
Published: December 24, 2014

REFERENCES

1000 Genomes Project Consortium, Abecasis, G.R., Altshuler, D., Auton, A., Brooks, L.D., Durbin, R.M., Gibbs, R.A., Hurles, M.E., and McVean, G.A. (2010). A map of human genome variation from population-scale sequencing. Nature *467*, 1061–1073.

Arumugaswami, V., Wu, T.T., Martinez-Guzman, D., Jia, Q., Deng, H., Reyes, N., and Sun, R. (2006). ORF18 is a transfactor that is essential for late gene transcription of a gammaherpesvirus. J. Virol. *80*, 9730–9740.

Aubry, V., Mure, F., Mariamé, B., Deschamps, T., Wyrwicz, L.S., Manet, E., and Gruffat, H. (2014). Epstein-barr virus late gene transcription depends on the assembly of a virus-specific preinitiation complex. J. Virol. *88*, 12825–12838.

Bauer-Mehren, A., Bundschus, M., Rautschka, M., Mayer, M.A., Sanz, F., and Furlong, L.I. (2011). Gene-disease network analysis reveals functional modules in mendelian, complex and environmental diseases. PLoS ONE *6*, e20284.

Brulois, K.F., Chang, H., Lee, A.S., Ensser, A., Wong, L.Y., Toth, Z., Lee, S.H., Lee, H.R., Myoung, J., Ganem, D., et al. (2012). Construction and manipulation of a new Kaposi's sarcoma-associated herpesvirus bacterial artificial chromosome clone. J. Virol. *86*, 9708–9720.

Bushnell, D.A., Westover, K.D., Davis, R.E., and Kornberg, R.D. (2004). Structural basis of transcription: an RNA polymerase II-TFIIB cocrystal at 4.5 angstroms. Science *303*, 983–988.

Calderwood, M.A., Venkatesan, K., Xing, L., Chase, M.R., Vazquez, A., Holthaus, A.M., Ewence, A.E., Li, N., Hirozane-Kishikawa, T., Hill, D.E., et al. (2007). Epstein-Barr virus and virus human protein interaction maps. Proc. Natl. Acad. Sci. USA *104*, 7606–7611.

Dorjsuren, D., Lin, Y., Wei, W., Yamashita, T., Nomura, T., Hayashi, N., and Murakami, S. (1998). RMP, a novel RNA polymerase II subunit 5-interacting protein, counteracts transactivation by hepatitis B virus X protein. Mol. Cell. Biol. *18*, 7546–7555.

Engelhardt, O.G., Smith, M., and Fodor, E. (2005). Association of the influenza A virus RNA-dependent RNA polymerase with cellular RNA polymerase II. J. Virol. *79*, 5812–5818.

Germain, M.A., Chatel-Chaix, L., Gagne, B., Bonneil, E., Thibault, P., Pradezynski, F., de Chassey, B., Meyniel-Shicklin, L., Lotteau, V., Baril, M., et al. (2013). Elucidating novel hepatitis C virus/host interactions using combined mass spectrometry and functional genomics approaches. Mol. Cell. Proteomics *13*, 184–203.

Gruffat, H., Kadjouf, F., Mariamé, B., and Manet, E. (2012). The Epstein-Barr virus BcRF1 gene product is a TBP-like protein with an essential role in late gene expression. J. Virol. *86*, 6023–6032.

Guglielmi, B., La Rochelle, N., and Tjian, R. (2013). Gene-specific transcriptional mechanisms at the histone gene cluster revealed by single-cell imaging. Mol. Cell *51*, 480–492.

Hirsch, A.J. (2010). The use of RNAi-based screens to identify host proteins involved in viral replication. Future Microbiol. *5*, 303–311.

Homa, F.L., Glorioso, J.C., and Levine, M. (1988). A specific 15-bp TATA box promoter element is required for expression of a herpes simplex virus type 1 late gene. Genes Dev. *2*, 40–53.

Isomura, H., Stinski, M.F., Murata, T., Yamashita, Y., Kanda, T., Toyokuni, S., and Tsurumi, T. (2011). The human cytomegalovirus gene products essential for late viral gene expression assemble into prereplication complexes before viral DNA replication. J. Virol. *85*, 6629–6644.

Jäger, S., Cimermancic, P., Gulbahce, N., Johnson, J.R., McGovern, K.E., Clarke, S.C., Shales, M., Mercenne, G., Pache, L., Li, K., et al. (2011a). Global landscape of HIV-human protein complexes. Nature *481*, 365–370.

Jäger, S., Gulbahce, N., Cimermancic, P., Kane, J., He, N., Chou, S., D'Orso, I., Fernandes, J., Jang, G., Frankel, A.D., et al. (2011b). Purification and characterization of HIV-human protein complexes. Methods *53*, 13–19.

Jia, Q., Wu, T.T., Liao, H.I., Chernishof, V., and Sun, R. (2004). Murine gammaherpesvirus 68 open reading frame 31 is required for viral replication. J. Virol. *78*, 6610–6620.

Kim, Y., Geiger, J.H., Hahn, S., and Sigler, P.B. (1993). Crystal structure of a yeast TBP/TATA-box complex. Nature *365*, 512–520.

Lee, S., Salwinski, L., Zhang, C., Chu, D., Sampankanpanich, C., Reyes, N.A., Vangeloff, A., Xing, F., Li, X., Wu, T.T., et al. (2011). An integrated approach to elucidate the intra-viral and viral-cellular protein interaction networks of a gamma-herpesvirus. PLoS Pathog. *7*, e1002297.

Listerman, I., Sapra, A.K., and Neugebauer, K.M. (2006). Cotranscriptional coupling of splicing factor recruitment and precursor messenger RNA splicing in mammalian cells. Nat. Struct. Mol. Biol. *13*, 815–822.

Maher, M.C., and Hernandez, R.D. (2014). A MOSAIC of methods: Improving ortholog detection through integration of algorithmic diversity. http://arxiv.org/abs/1309.2319.

Mavankal, G., Ignatius Ou, S.H., Oliver, H., Sigman, D., and Gaynor, R.B. (1996). Human immunodeficiency virus type 1 and 2 Tat proteins specifically interact with RNA polymerase II. Proc. Natl. Acad. Sci. USA *93*, 2089–2094.

Mesri, E.A., Feitelson, M.A., and Munger, K. (2014). Human viral oncogenesis: a cancer hallmarks analysis. Cell Host Microbe *15*, 266–282.

Murakami, K., Elmlund, H., Kalisman, N., Bushnell, D.A., Adams, C.M., Azubel, M., Elmlund, D., Levi-Kalisman, Y., Liu, X., Gibbons, B.J., et al. (2013). Architecture of an RNA polymerase II transcription pre-initiation complex. Science *342*, 1238724.

Myoung, J., and Ganem, D. (2011). Generation of a doxycycline-inducible KSHV producer cell line of endothelial origin: maintenance of tight latency with efficient reactivation upon induction. J. Virol. Methods *174*, 12–21.

Navratil, V., de Chassey, B., Combe, C.R., and Lotteau, V. (2011). When the human viral infectome and diseasome networks collide: towards a systems biology platform for the aetiology of human diseases. BMC Syst. Biol. *5*, 13.

Österberg, S., del Peso-Santos, T., and Shingler, V. (2011). Regulation of alternative sigma factor use. Annu. Rev. Microbiol. *65*, 37–55.

Perng, Y.C., Campbell, J.A., Lenschow, D.J., and Yu, D. (2014). Human cytomegalovirus pUL79 is an elongation factor of RNA polymerase II for viral gene transcription. PLoS Pathog. *10*, e1004350.

Pichlmair, A., Kandasamy, K., Alvisi, G., Mulhern, O., Sacco, R., Habjan, M., Binder, M., Stefanovic, A., Eberle, C.A., Goncalves, A., et al. (2012). Viral immune modulators perturb the human molecular network by common and unique strategies. Nature *487*, 486–490.

Ramage, H.R., Kumar, G.R., Verschueren, E., Johnson, J.R., Von Dollen, J., Johnson, T., Newton, B., Shah, P., Horner, J., Krogan, N.J., and Ott, M. (2015). A combined proteomics/genomics approach links hepatitis C virus infection with nonsense-mediated mRNA decay. Mol. Cell *57*, this issue, 329–340.

Rajagopala, S.V., Casjens, S., and Uetz, P. (2011). The protein interaction map of bacteriophage lambda. BMC Microbiol. *11*, 213.

Rozenblatt-Rosen, O., Deo, R.C., Padi, M., Adelmant, G., Calderwood, M.A., Rolland, T., Grace, M., Dricot, A., Askenazi, M., Tavares, M., et al. (2012). Interpreting cancer genomes using systematic host network perturbations by tumour virus proteins. Nature *487*, 491–495.

Smoot, M.E., Ono, K., Ruscheinski, J., Wang, P.L., and Ideker, T. (2011). Cytoscape 2.8: new features for data integration and network visualization. Bioinformatics *27*, 431–432.

Sturzl, M., Gaus, D., Dirks, W.G., Ganem, D., and Jochmann, R. (2013). Kaposi's sarcoma-derived cell line SLK is not of endothelial origin, but is a contaminant from a known renal carcinoma cell line. Int. J. Cancer *132*, 1954–1958.

Swift, S., Lorens, J., Achacoso, P., and Nolan, G.P. (2001). Rapid production of retroviruses for efficient gene delivery to mammalian cells using 293T cell-based systems. Curr. Protoc. Immunol. *Chapter 10*. Unit 10.17C. http://dx.doi.org/10.1002/0471142735.im1017cs31.

Szpiech, Z.A., and Hernandez, R.D. (2014). selscan: an efficient multithreaded program to perform EHH-based scans for positive selection. Mol. Biol. Evol. *31*, 2824–2827.

Takramah, D., Seiffert, B.M., Schaller, S., Vigneron, M., and Häcker, G. (2003). Baculovirus P35 interacts with a subunit of human RNA polymerase II and can enhance promoter activity in human cells. J. Gen. Virol. *84*, 3011–3019.

Tang, S., Yamanegi, K., and Zheng, Z.M. (2004). Requirement of a 12-base-pair TATT-containing sequence and viral lytic DNA replication in activation of the Kaposi's sarcoma-associated herpesvirus K8.1 late promoter. J. Virol. *78*, 2609–2614.

Thomas, M.C., and Chiang, C.M. (2006). The general transcription machinery and general cofactors. Crit. Rev. Biochem. Mol. Biol. *41*, 105–178.

Uetz, P., Dong, Y.A., Zeretzke, C., Atzler, C., Baiker, A., Berger, B., Rajagopala, S.V., Roupelieva, M., Rose, D., Fossum, E., and Haas, J. (2006). Herpesviral protein networks and their interaction with the human proteome. Science *311*, 239–242.

Vance, R.E., Isberg, R.R., and Portnoy, D.A. (2009). Patterns of pathogenesis: discrimination of pathogenic and nonpathogenic microbes by the innate immune system. Cell Host Microbe *6*, 10–21.

Voight, B.F., Kudaravalli, S., Wen, X., and Pritchard, J.K. (2006). A map of recent positive selection in the human genome. PLoS Biol. *4*, e72.

Wong, E., Wu, T.T., Reyes, N., Deng, H., and Sun, R. (2007). Murine gammaherpesvirus 68 open reading frame 24 is required for late gene expression after DNA replication. J. Virol. *81*, 6761–6764.

Wong-Ho, E., Wu, T.T., Davis, Z.H., Zhang, B., Huang, J., Gong, H., Deng, H., Liu, F., Glaunsinger, B., and Sun, R. (2014). Unconventional sequence requirement for viral late gene core promoters of murine gammaherpesvirus 68. J. Virol. *88*, 3411–3422.

Wu, T.T., Park, T., Kim, H., Tran, T., Tong, L., Martinez-Guzman, D., Reyes, N., Deng, H., and Sun, R. (2009). ORF30 and ORF34 are essential for expression of late genes in murine gammaherpesvirus 68. J. Virol. *83*, 2265–2273.

Wyrwicz, L.S., and Rychlewski, L. (2007). Identification of Herpes TATT-binding protein. Antiviral Res. *75*, 167–172.

Zhou, C., and Knipe, D.M. (2002). Association of herpes simplex virus type 1 ICP8 and ICP27 proteins with cellular RNA polymerase II holoenzyme. J. Virol. *76*, 5893–5904.